THERMO-FLUID MECHANICS OF LIQUID OR GAS COOLED TUBULAR FIRST WALLS

J. A. FILLO, J. R. POWELL

Brookhaven National Laboratory, Department of Nuclear Energy, Upton, New York 11973, U.S.A.

Abstract

In the development of fusion reactors, the ability to cool the first wall looms as a critical region of concern. A number of ideas have been set forth to accommodate the high heat fluxes and neutron and gamma heat generation in the first wall. A feature common to several of the ideas is an array of tubes or tube bank forming a first wall shield.

The attendant heat transfer problem for single phase fluids is that of turbulent heat transfer in a circular tube with variable circumferential heat flux and volumetric neutron-gamma heat generation in the tube wall and coolants--such as water.

An analysis for hydrodynamically and thermally, fully developed heat transfer in a circular tube coupled with heat conduction in the tube wall is presented. Anisotropy of turbulent energy transport has been taken into account employing theoretical results for eddy diffusivity in the various directions. Assumptions such as thin-walled structures where radial temperature gradients are negligible and/or constant heat transfer coefficients are relaxed are shown to be special cases of this analysis. The energy equations for the fluid and solid body are solved simultaneously and are subject to continuity in heat flux and temperature at the interface. Circumferential as well as radial temperature gradients are permitted in both energy equations along with internal heat generation in the tube wall and fluid. Solutions of the equations are found by a method of separation-of-variables. We restrict ourselves to cases where the applied surface heat flux may be expressed in terms of a sine-cosine Fourier series.

Indicative of the analysis but by no means the only conclusion reached is that neglecting radial conduction but allowing circumferential conduction results in underestimating the wall temperature for relatively thin-walled structures (for the set of design conditions studied). This also implies that the fluid temperature is underestimated. The difference in maximum tube wall temperature is attributed to the fact that the temperature is proportional to the average heat flux multiplied by the inner tube radius, whereas in the complete analysis, it is the average heat flux multiplied by the outer tube radius. Results differ approximately in proportion to the ratio of outer to inner tube radii (R_o/R_i) so that multiplying the inner wall temperature by R_o/R_i brings the two results together.

In addition a comparison of the dimensionless tube wall temperature equation derived from the coupled analysis with that based on a constant heat transfer coefficient indicates that the constant heat transfer analysis can be made identical with the current case by renormalizing the heat transfer coefficient.

In summary the analysis, with minimal assumptions, provides the designer with a simple set of analytical design equations for the coupling of solid and fluid temperature distributions for obtaining the Nusselt numbers. A guide to modify results based on thin wall approximations and a constant heat transfer coefficient for cases when these assumptions do not hold is also indicated.

*Work performed under the auspices of the United States Department of Energy.

1. Introduction

All of the emissions from a reacting D-T plasma may intersect the first wall of a fusion reactor. These include ions and neutral particles, primary neutrons, X-rays (bremsstrahlung), and cyclotron radiation. In addition, scattered neutrons and gamma radiation generated in the blanket regions exterior to this first wall are also imposed on it. Finally, D-T gas surrounding the plasma may react chemically with the first wall materials. One result of these many interactions is the generation of appreciable heat which can be up to 20% of the plasma output. In most analyses the above effects are usually lumped together as a radiant flux. While the incident fluxes are absorbed in a small depth of any first wall material, the usual assumption is to treat the lumped radiant flux as if it were deposited on the first wall surface. In heat transfer analyses it is an applied heat flux boundary condition. A number of ideas have been set forth to accommodate the high heat fluxes and neutron and gamma heat generation in the first wall as well as high energy fluxes which may also arise from neutral beam injectors. A feature common to several of the ideas is an array of tubes or tube bank forming a first wall shield.

The attendant heat transfer problem for single phase fluids is that of turbulent heat transfer in a circular tube with variable circumferential heat flux, volumetric neutron-gamma heat generation in the tube wall, and a coolant such as water. Theoretical work allowing for a nonuniform heat flux distribution around the circumference of a circular tube for both fully developed laminar and turbulent flow has been considered by REYNOLDS [1,2,3,], SPARROW and LIU [4], RAPIER [5], GARTNER, et.al [6], and most recently by FILLO and POWELL [7]. The current work is an extension of [7] to include: a) volumetric heat generation in a coolant; and b) a comparison of tube wall temperatures based on a varying heat transfer coefficient and a constant coefficient.

2. Coupled Conduction-Convection Equations

For the case of single phase fluids in a circular duct, we consider hydrodynamically, fully developed turbulent flow. Thermal properties of the fluid are taken to be constant. The fluid temperature field is also assumed to be fully developed. Anisotropy of turbulent energy transport has been taken into account employing theoretical results, GARTNER [6], for eddy diffusivity in the radial and circumferential directions. For an applied heat flux with arbitrary circumferential variation at the outer tube wall (see Figure 1), but invariant in the flow direction, the temperature distributions in the tube wall and fluid are to be determined. Both radial and circumferential temperature variations are permitted. The energy equations for the temperatures in the tube wall and fluid are solved simultaneously, subject to continuity conditions in heat flux and temperature at the interface. Internal heat generation is permitted in the tube wall, but it is assumed constant, i.e., averaged over the tube thickness. Likewise, internal heat generation in the coolant is allowed but assumed constant and averaged over the inner tube diameter. The governing conduction equation for the tube is:

$$L_s(\theta_s) + Q_s = 0 \qquad (1)$$

subject to the boundary conditions:

$$\lambda_s \frac{\partial \theta_s}{\partial r} \Big)_{R_o} = \dot{q}(\phi) \tag{2a}$$

$$-\lambda_s \frac{\partial \theta_s}{\partial r} \Big)_{R_i} = -\lambda_f \frac{\partial \theta_f}{\partial r} \Big)_{R_i} \tag{2b}$$

$$\theta_s(R_i, \theta) = \theta_f (R_i, x, \phi) \tag{2c}$$

in addition to:

$$\theta_s(r, \phi) = \theta_s (r, \phi, + 2\pi) \tag{3a}$$

$$\frac{1}{r} \frac{\partial \theta_s}{\partial \phi} (r, \phi) = \frac{1}{r} \frac{\partial \theta_s}{\partial \phi} (r, \phi+2\pi) \tag{3b}$$

The first boundary condition, eq. (2a), is applied heat flux and is prescribed to vary in an arbitrary manner at the outer wall of the tube. It is represented by:

$$\dot{q} (\phi) = \dot{q}_o + F(\phi) \tag{4a}$$

where

$$\int_o^{2\pi} F(\phi) \, d\phi = 0 \tag{4b}$$

Equation (2b) matches the heat flux at the boundary between solid and fluid and allows for the coupling between the governing equations in the tube wall and fluid. Equation (2c) assumes continuity of temperatures at the interface; eqs. (3a) and (3b) satisfy the condition that the temperature in the tube will be single-valued.

The mean thermal energy equation governing the fluid is:

$$L_f(\theta_f) \quad -u \frac{\partial \theta_f}{\partial x} + \frac{Q_f}{\rho c_p} = 0 \tag{5}$$

Since the temperature, θ_f, appears only as the first power in eq. (5), superposition of solutions to a linear equation is applied. In particular we separate the general problem into the following two problems: (1) a fluid with no internal heat generation ($Q_f = 0$) flowing in a duct with heat transfer at the tube half, the temperature distribution denoted by $\theta_{f,q}$; and (2) a fluid with internal heat generation, Q_f, flowing in a duct with insulated walls, the temperature distribution denoted by $\theta_{f,Q}$. Consequently, the solution to eq. (5) may be written as:

$$\theta_f = \theta_{f,q} + \theta_{f,Q} \tag{6}$$

The equations and boundary conditions for $\theta_{f,q}$ and $\theta_{f,Q}$ are, respectively:

$$L_f(\theta_{f,q}) - u\frac{\partial\theta_{f,q}}{\partial x} = 0 \qquad (7)$$

$$-\lambda_s \frac{\partial\theta_{s,q}}{\partial r})R_i = -\lambda_f \frac{\partial\theta_{f,q}}{\partial r})R_i \quad * \qquad \theta_{s,q}(R_i, \phi) = \theta_{f,q}(R_i, x, \phi)$$

$$\theta_{f,q}(0, x, \phi) = \theta_{f,qm}(x) \qquad \theta_{f,q}(r, 0, \phi) = T_0 \qquad (7a)$$

and

$$L_f(\theta_{f,Q}) - u\frac{\partial\theta_{f,Q}}{\partial x} + \frac{Q_f}{\rho c_p} = 0 \qquad (8)$$

$$\frac{\partial\theta_{f,Q}}{\partial r})_{R_i} = 0 \qquad \theta_{s,Q}(R_i, \phi) = \theta_{f,Q}(R_i, x, \phi)$$

$$\theta_{f,Q}(0, x, \phi) = \theta_{f,Qm}(x) \qquad \theta_{f,Q}(r, 0, \phi) = T_o \quad ** \qquad (8a)$$

The equations for $\theta_{s,q}$ and $\theta_{s,Q}$ and boundary conditions become:

$$L_s(\theta_{s,q}) + Q_s = o \qquad (9)$$

and

$$\lambda_s \frac{\partial\theta_{s,q}}{\partial r})R_o = \dot{q}(\phi) \qquad (9a)$$

as well as the matching heat flux and temperature continuity conditions specified by eq. (7a). Conditions as in eq. (3a) and (3b) are likewise satisfied by $\theta_{s,q}$.
In addition the following conditions apply:

$$L_s(\theta_{s,Q}) = 0 \qquad (10)$$

subject to

$$\frac{\partial\theta_{s,Q}}{\partial r})_{R_o} = 0 \qquad (10a)$$

and conditions specified by eqs. (8a), (3a), and (3b).

---

* As a consequence of splitting the fluid temperature into two superposable solutions and coupling the tube wall and fluid temperatures through the interface boundary conditions, the temperature for the solid (since the conduction equation is linear) is likewise split into two superposable solutions. ** For a combined coolant heat source and wall heat transfer problem, separate problems for $\theta_{f,Q}$ and $\theta_{f,q}$ cannot both have entering temperatures of T_o. If T_o is specified for $\theta_{f,q}$ then $\theta_{f,}$ (r, 0, ϕ) = 0.

3. Solutions to Energy Equations

3.1 Heat Transfer at the Tube Wall

The solutions to eq. (7) subject to boundary conditions (7a) as well as eqs. (9) and (9a) have been found previously, FILLO and POWELL [7].

3.2 Insulated Wall

Because of the zero gradient boundary conditions at both $r = R_o$ and R_i, the solution for $\theta_{s,Q}$, which satisfies eq. (10) and the boundary conditions is:

$$\theta_{s,Q} = \text{constant}. \tag{11}$$

The constant is to be determined from the matching conditions with $\theta_{f,Q}$ at the solid-fluid interface.

The implication from $\theta_{s,Q}$ = a constant is that $\theta_{f,Q}$ does not vary with ϕ, i.e., $\theta_{f,Q}$ may be written as:

$$\theta_{f,Q}(\xi, x, \phi) = \theta_{f,Qm}(x) + Q_f R_i^2/\lambda_f \Phi(\xi) \tag{12}$$

where Φ is the temperature field associated with the internal heat generation, Q_f, in the fluid. It is dependent on a particular form of the velocity profile, U, as well as eddy diffusivity in the radial direction. The equation governing Φ is

$$\frac{d}{d\xi}\left[L_\xi(\xi)\ \xi\ \frac{d\Phi}{d\xi}\right] + \xi(1-U) = 0 \tag{13}$$

subject to boundary conditions:

$$\Phi(0) = 0 \text{ and } \left(\frac{d\Phi}{d\xi}\right)_1 = 0. \tag{13a}$$

The mixed mean temperature, $\theta_{f,Qm}$, based on Q_f is defined as:

$$\theta_{f,Qm} = \frac{1}{A_i U_m}\int_{A_i} u\theta_{f,Q}\,dA \tag{14}$$

and is determined from an overall energy balance on the fluid, i.e.,

$$\frac{d\theta_{f,Qm}}{dx} = \frac{Q_f}{\rho U_m c_p} \tag{15}$$

3.3 Comparison of Results for Constant Heat Transfer Coefficient, h, and the Present Analysis

For the case of heat transfer at the tube wall but no volumetric energy generation in the coolant, and an applied heat flux, $\dot{q}$, which varies as:

$$\dot{q} = \dot{q}_o(1 + \cos\phi). \tag{16}$$

The temperature distribution from FILLO and POWELL [7] in dimensionless form, becomes:

$$\frac{\theta_{s,q} - \theta_{f,qm}}{P/\lambda_s} = \frac{\lambda_s}{\lambda_f} g_o(1) + \ln r/R_i + \psi_1 \left[\ln r/R_i + \frac{1}{2}(1-(r/R_i)^2)\right] +$$

$$\frac{\delta^*}{\lambda_s/\lambda_f R_1(1)\ (1-\delta^{*2}) + 1 + \delta^{*2}} \left[\lambda_s/\lambda_f R_1(1) + 1)\ r/R_i\right. \qquad (17)$$

$$\left. + (\lambda_s/\lambda_f R_1(1) - 1)\ (r/R_i)^{-1}\right] \psi_2 \cos \Phi$$

where

$$\psi_1 = \frac{\delta^{*2}}{2(\dot{q}_o/R_o Q) + 1 - \delta^{*2}} \qquad \text{and} \qquad \psi_2 = \frac{1}{1 + (1 - \delta^{*2})QR_o/2\dot{q}_o}$$

Assuming that the boundary condition, eq. (2b), can be specified in terms of a constant heat transfer coefficient, h, i.e.,

$$\lambda_s \frac{\partial \theta_s}{\partial r}\Big)_{R_i} = h[\theta_f(R_i, \theta) - \theta_{f,m}] \qquad (18)$$

The dimensionless tube wall temperature becomes:

$$\frac{\theta_{s,q} - \theta_{f,qm}}{P/\lambda_s} = \frac{\lambda_s}{\lambda_f}(\lambda_f/hR_i) + \ln r/R_i + \psi_1[\ln r/R_i + \frac{1}{2}(1 - (r/R_i)^2] \qquad (19)$$

$$+ \frac{\delta^*}{\lambda_s/hR_i(1 - \delta^{*2}) + 1 + \delta^{*2}} \left[\lambda_s/hR_i + 1)\ r/R_i + (\lambda_s/hR_i - 1)(r/R_i)^{-1}\right] \psi_2 \cos \phi$$

Comparing eqs. (17) and (19), it is quite clear what terms are affected by relaxing the conditions of constant heat transfer coefficients. If h is defined to be the average heat transfer coefficient based on the average heat flux, $\dot{q}_o$, then $g_o(1)$ is related to h through

$$g_o(1) = \lambda_f/hR_i \qquad (20)$$

The numerical results from the analyses will then differ depending on the differences between $g_o(1)$ and $R_i(1)$. Differences can also arise as a consequence of using different predictions for velocity and eddy diffusivity distribution.

4. Discussion

For a given coolant and average temperature rise along the duct, the inside pipe diameter is fixed by choosing a reasonable average coolant velocity, pressure, and Reynolds number. In the case of helium it was assumed that the fluid velocity in the tube was 30 m/s which is typical of fluid velocities in the core coolant holes of a standard HTGR and in the regeneration tubes of a direct-cycle HTGR. The pressure was assumed to be 50 atm. For the

water coolant case, it was assumed that the average velocity was 5 m/s, sufficiently low to inhibit corrosion in the stainless steel or aluminum tubes while a pressure of $\sim$ 60 atm was considered high enough to suppress boiling in the first wall.

The coolant temperature rise depends on the mass flow rate (fixed by the pressure, average coolant velocity, and inside pipe diameter), the length of the tube, and the wall loading. While the coolant circuit can be arranged so that the coolant temperature is raised from the coolant inlet temperature to the maximum desirable outlet temperature within the first wall itself, or the first wall coolant temperature rise could be only a fraction of the total in a system in which the coolant leaving the first wall would then enter the blanket, practical constraints are placed on tube lengths, i.e., fabrication, size of blanket modules, maintenance, etc. Fixing the bulk or mean temperature, mass flow rate, and wall loading fixes the tube length. Since the tube length is inversely proportional to wall loading, the tube length decreases with an increase in wall loading.

In the case of helium, for a fixed mean temperature rise and Reynolds number, the inside diameter increases as the average coolant temperature increases whereas for water, for the same thermal conditions but slightly higher Reynolds number, the inside diameter decreases. The diameter for the water-cooled cases are factors of 3-4 less while the tube lengths are a factor of 8 greater than for helium. The effect of an increase in the tube wall thickness is to decrease the tube length.

The helium conditions, $\Delta\theta_{fm} \geq 200^{o}C$, $\theta_{avg} > 500^{o}C$ are for SiC tubes whereas the other cases (water included) are for aluminum and stainless steel. The helium cooled SiC tube lengths are quite excessive at the higher Reynolds numbers, especially for $\Delta\theta_{fm} > 200^{o}C$, $\theta_{avg} > 500^{o}C$, as are the tube lengths for the water-cooled cases. At a higher wall load, i.e., 3 MW(th)/m^2, the tube lengths decrease by a factor of three.

Tube wall steady-state temperature profiles (temperature difference above the mean fluid temperature) shown in Figures 2 and 3 are comparisons between aluminum and stainless steel tubes for $\phi = 0$, i.e., where maximum heat flux occurs. The contribution of volumetric heating of water to the tube wall temperature is negligible, i.e. $\lesssim 1^{o}C$, as well as to the temperature difference between the tube wall and coolant. For example, at the Reynolds number of interest, $Re = 3 \times 10^{5}$, and Prandtl number, $P_r \sim 1$, the dimensionless temperature function, $\Phi(R_i) \sim 6 \times 10^{-5}$, and the tube wall-coolant temperature difference is:

$$\theta_{f,Q}(R_i) - \theta_{f,Qm} = 1.57\ Q_f \times 10^{-3}$$

In other words the volumetric heating of the coolant would have to be several orders of magnitude greater and/or the flow at a much lower Reynolds number since Φ increases with a decreasing Reynolds number (and decreasing Prandtl number). In general at a fixed Reynolds number, a lower Prandtl number fluid will make a larger contribution to the tube wall-coolant temperature due to volumetric heating.

The results in Figures 2 and 3 reflect the decreased temperature gradient across the tube wall as well as decreased temperature for a high thermal conductivity material such as aluminum. For either the helium or water-cooled cases, the maximum temperature difference across the tube wall can be correlated with $X\delta/\lambda_s$, i.e.,

$$\Delta\theta_s = 0.12\ X\delta/\lambda_s \qquad (21)$$

where χ is the wall load.
This reconfirms the results found in reference [8], derived solely for a helium-cooled SiC tube, finite difference analysis, and somewhat different boundary conditions.

The maximum tube surface temperature depends both on the temperature difference across the wall and the temperature drop across the coolant boundary layer. These two effects are reflected in the figures. The maximum temperature for stainless steel is greater than that of aluminum by virtue of its lower thermal conductivity. The maximum temperatures for the water-cooled cases are lower since the thermal conductivity of water is greater than that of helium at the same corresponding average coolant temperature.

Increasing the average coolant temperature by 100°C raises the inside wall temperature a few degrees and the maximum surface temperature $\sim$ 15°C for both the helium and water-cooled cases. By increasing the tube wall thickness from 0.3 cm to 0.5 cm, the maximum surface temperature of stainless increases $\sim$ 10°C while the aluminum surface temperature increases a few degrees.

The effect on the maximum surface and wall temperatures, assuming a constant heat transfer coefficient, is shown by comparing eqs. (17) and (19). A comparison of the g_o and R_1 values found in GARTNER [6] shows that at low Prandtl numbers, in the liquid metal range, the ratio of $g_o/R_1 \sim 0.3$ whereas in the cases of helium and water $g_o/R_1 \sim 0.7$-0.8. In other words the difference between the two analyses would be more noticeable at lower Prandtl numbers. A closer examination of the g_o and R_1 values for the helium and water cases shows that the g_o and R_1 values tend to be closer with increasing Reynolds and higher Prandtl numbers, explaining why the small yet different values for the helium and water cases are observed when the constant heat transfer coefficient analysis and current analysis are compared.

Here, implicitly, we've assumed that h is the average heat transfer coefficient, related to g_o by eq. (22). If h were calculated from the Dittus-Boelter correlation or from the analysis of REYNOLDS [2] or SUTHERLAND and KAYS [9], the discrepancy between the two analyses would be more noticeable.

As in FILLO and POWELL [7], it is reconfirmed that allowing circumferential conduction but neglecting radial conduction underestimates the maximum wall temperature. The difference is attributed to the fact that the temperature is proportional to the average heat flux multiplied by the inner tube radius (neglecting radial conduction) whereas including radial conduction it is the average heat flux multiplied by the outer tube radius which determines the maximum surface temperature.

5. References

/1/ REYNOLDS, W. C., Transactions ASME, Vol. 82, No. 2, p. 108-112 (1960).

/2/ REYNOLDS, W. C., Intl. J. of Heat and Mass Transfer, Vol. 6, p. 445-454 (1963).

/3/ REYNOLDS, W. C., Intl. J. of Heat and Mass Transfer, Vol. 6, p. 925 (1963).

/4/ SPARROW, E. M., LIU, S. H., Intl. J. of Heat and Mass Transfer, Vol. 6, p. 866-867 (1963).

/5/ RAPIER, A. C., Intl. J. of Heat and Mass Transfer, Vol. 15, p. 527-538 (1972).

/6/ GARTNER, D., JOHANNSEN, K., RAMM, H., Intl. J. of Heat and Mass Transfer, Vol. 17, p. 1003-1013 (1974).

/7/ FILLO, J. A., POWELL, J. R., Sixth Intl. Heat Transfer Conf., EC-30, Toronto, Canada (1978).

/8/ GENERAL ATOMIC, CORP., Fusion Reactor Design Studies, GA-A13430 (1975).

/9/ SUTHERLAND, W. A., and KAYS, W. M., Intl. J. of Heat and Mass Transfer, Vol. 7, p. 1187-1194 (1964).

6. Nomenclature

A_n, a_n, B_n, b_n, c_n, d_n, e_n, f_n = Fourier Coefficients

A_i = inside tube area, πR_i^2, m^2

A_w = solid tube area, $\pi (R_o^2 - R_i^2)$, m^2

c_p = specific heat at constant pressure, J/kgK

E = diffusivity function, $(1+K/\kappa)$

K = eddy thermal diffusivity, m^2/s

L = tube length, m

L_s = operator, $\lambda_s \left[\frac{1}{r}\frac{\partial}{\partial r}\left(r\frac{\partial}{\partial r}\right) + \frac{1}{r^2}\frac{\partial^2}{\partial \phi^2}\right]$

L_f = operator, $\kappa \left[\frac{1}{r}\frac{\partial}{\partial r}\left(rE_r\frac{\partial}{\partial r}\right) + \frac{1}{r^2}\frac{\partial}{\partial \phi}\left(E_\phi\frac{\partial}{\partial \phi}\right)\right]$

L_f^* = dimensionless operator, $\frac{1}{\xi}\frac{\partial}{\partial \xi}\left(\xi E_\xi \frac{\partial}{\partial \xi}\right) + \frac{1}{\xi^2}\frac{\partial}{\partial \phi}\left(E_\phi\frac{\partial}{\partial \phi}\right)$

Nu = Nusselt number

P = $(P_o \dot{q}_o + A_w Q)/2\pi$, W/m

P_o = outside tube circumference, $2\pi R_o$, m

Pr = Prandtl number

$\dot{q}$ = applied surface heat flux, W/m^2

Q = average volumetric heating, W/m^3

r = radial co-ordinate, m

R = tube radius, m

R_n = radial temperature function

Re = Reynolds number

S = dimensionless temperature function

u = axial velocity, m/s

U = dimensionless velocity, u/U_m

x = axial co-ordinate, m

α = heat transfer coefficient, W/m^2K

δ = tube-wall thickness, m

$\delta^* = R_i/R_o$

η = dynamic viscosity, kg/ms

θ = temperature, ^oC

κ = thermal diffusivity, m^2/s

λ = thermal conductivity, W/mK

ξ = dimensionless radius, r/R_i

ρ = mass density, kg/m^3

Subscripts

f = fluid

i = inside

m = mixed mean

o = outside

s = solid

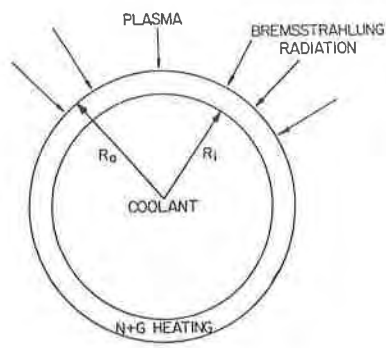

FIGURE 1 Heat Deposition in Tube

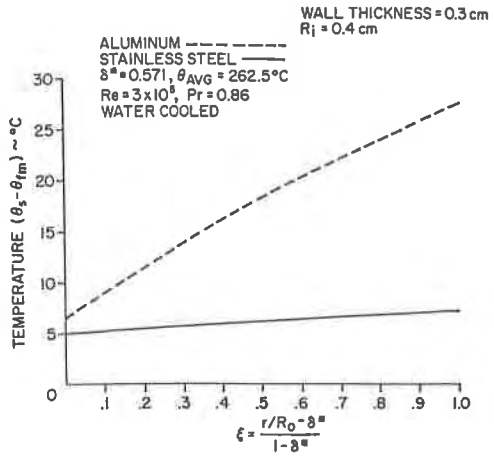

FIGURE 2 Radial Temperature Distribution in Tube Wall

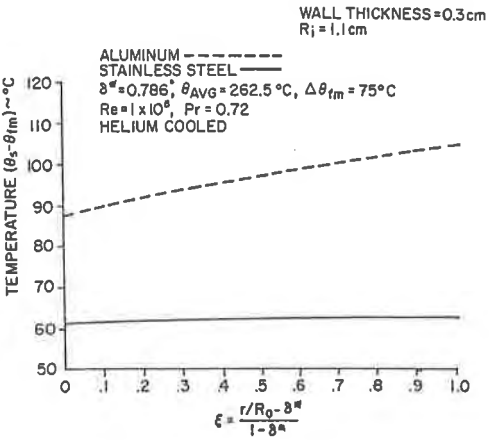

FIGURE 3 Radial Temperature Distribution in Tube Wall